20.   THE EFFECT OF CLAY ON POROSITY AND RESISTIVITY LOGS

20.1   Introduction

The presence of clay minerals or shale in porous formations presents problems from the interpretation of wireline logs. For most logs these problems have been discussed in the relevant chapter. The problem is, however, especially bad in the interpretation of resistivity data, and also affects the porosity logs. This is not only because the presence of clays and shale have a gross effect upon resistivity values, but because such data effects the final calculated STOOIP for a given formation. Even small amounts of clay can have a large effect, which is important because most reservoir sands contain some degree of shaliness.

Note: The terms clay and shale are used interchangeably by petrophysicists.

The distribution of clay within porous reservoir formations can be classified into three groups:

* Laminated – thin layers of clay between sand units.
* Structural – clay particles constitute part of the rock matrix, and are distributed within it. An example of this is coprolites.
* Dispersed – clay in the open spaces between the grains of the clastic matrix.

These are depicted schematically in Fig. 20.1.
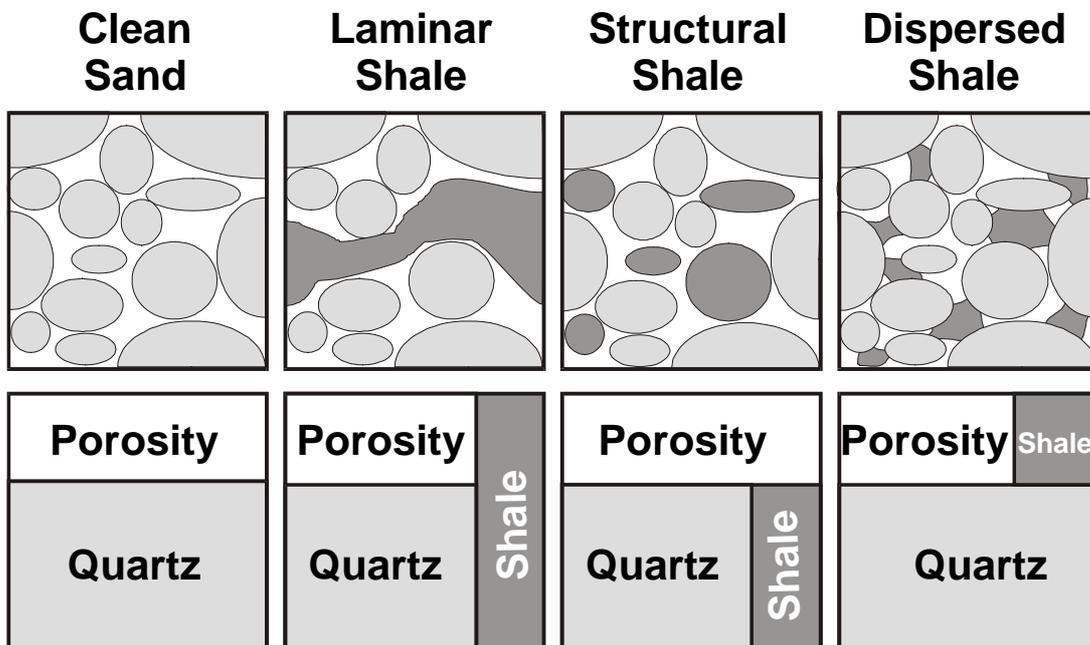
Fig. 20.1 Different modes of clay distribution in a reservoir.

The laminated and structural clays are part of the rock structure and are considered to have the same porosity (water content) as adjacent clay beds because they were subjected to the same overburden pressures. By contrast, the dispersed clays were only subjected to the formation fluid pressure, and therefore have a higher porosity and water content.

20.2 Porosity Logs

There are two different types of porosity that are relevant:

- Total porosity.

- Effective porosity.

These are illustrated in Fig. 20.2.
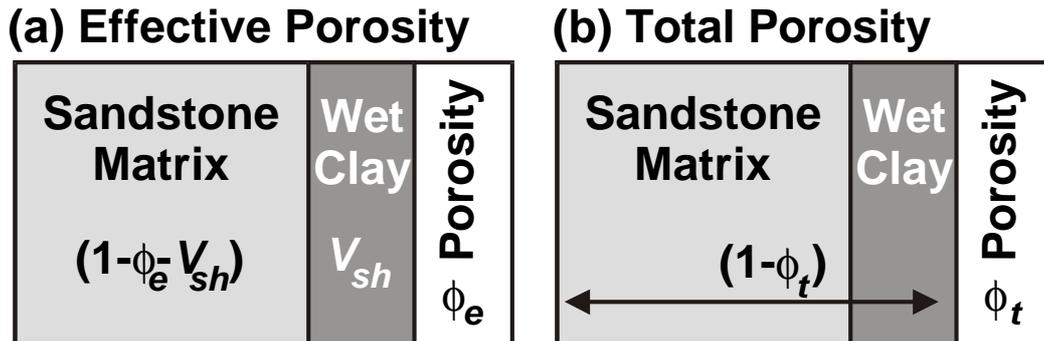
Fig. 20.2 Porosity models. (a) Total porosity. (b) Effective porosity.

20.2.1 Effective Porosity

The bulk volume of the rock is composed of a clastic/carbonate matrix fraction, a wet clay fraction (V_{sh}), and an "effective porosity", f_e. The matrix is therefore $(1 - V_{sh} - f_e)$. This model is the basis for the density – neutron cross-plots, which is commonly used to assess f_e and V_{sh} in shaly formations, using the following equations:

$$r_b = \left((1 - f_e - V_{sh}) \times r_{ma}\right) + \left(f_e \times r_e\right) + \left(V_{sh} \times r_{sh}\right) \tag{20.1}$$

$$f_N = f_e + V_{sh} \times f_{sh} \tag{20.2}$$

Figure 20.3 illustrates this method graphically. The graph is a triangle, whose apices are at the following points:

- The clean matrix point: $f_N = 0\%$ $r_b = 2.65$ g/cm^3
- The fluid point: $f_N = 100\%$ $r_b = 1.00$ g/cm^3
- The clean matrix point: f_N and r_b obtained from an adjacent clay

The linear effective porosity scale is shown on the matrix-water side and the clay-water side. The iso-V_{sh} lines are drawn across the triangle. Each pair of f_N and r_b values obtained from the logs can be entered into the graph and the relevant effective porosity and V_{sh} can be read off. Alternately, a more accurate figure can be obtained by solving Eqs. (20.1 and 20.2).
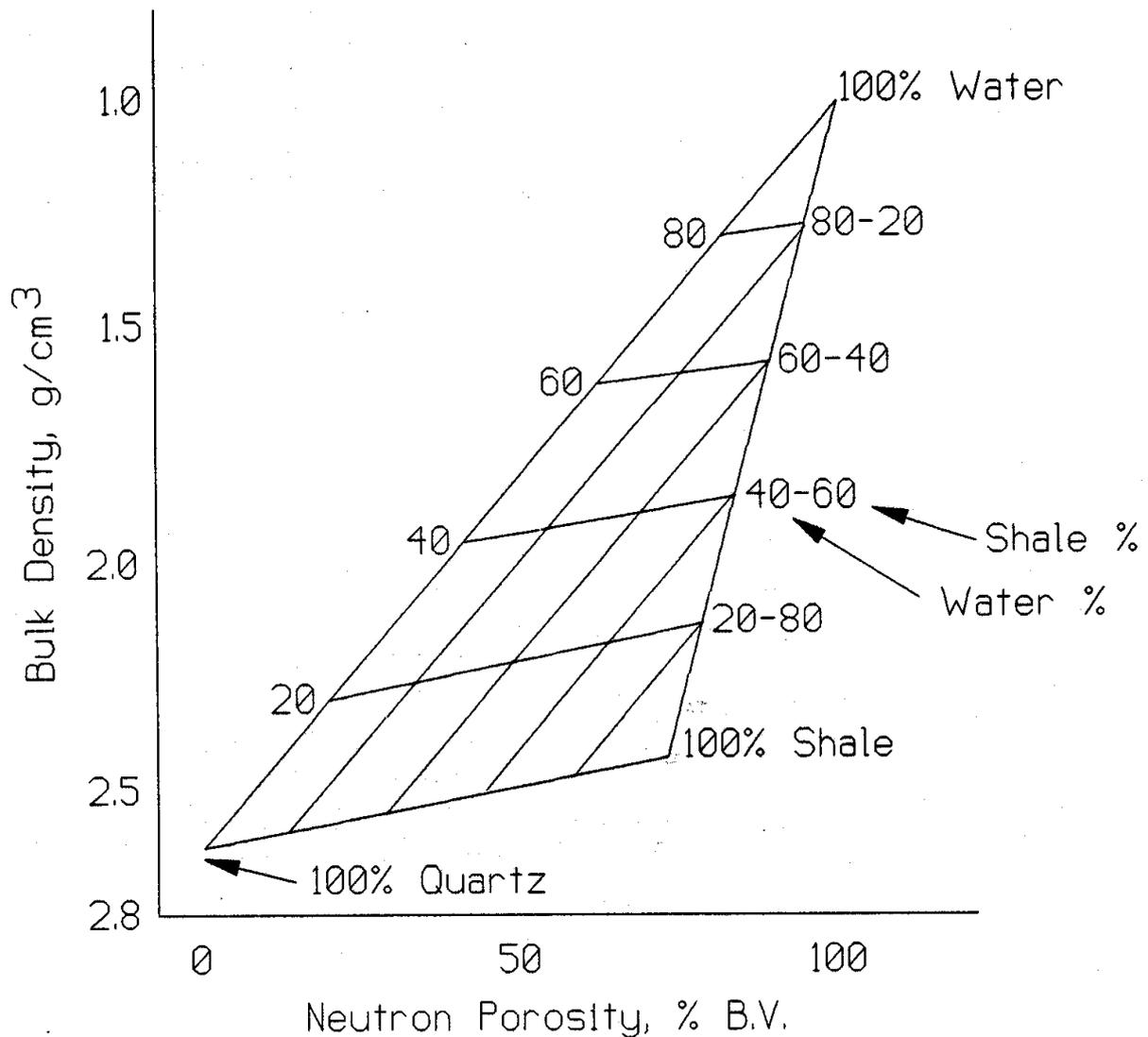
Fig. 20.3 Porosity- V_{sh} correction chart for the density – neutron log combination.

20.2.2 Total Porosity

In the total porosity mode, the clay grains/crystals are assumed to have a grain density equal to that of quartz. This is actually a good approximation for illite, kaolinite and montmorillonite. The model is composed of a sandstone matrix fraction, a clay crystal fraction (described as dry clay, i.e., without the clay bound water), and a so-called "total porosity" f_t. The matrix and dry clay fraction have a fraction $(1 - f_t)$. The value of f_t can be derived directly from the density log.

The porosity obtained from routine core analysis is also the total porosity in the sense that the procedures used to prepare the cores ensure that all oil is extracted from the cores, and the core is then dried. Under these conditions all absorbed and interstitial water is removed from the clay. As a result, there is often good agreement between routine core porosities and density log derived porosity data. If there is a discrepancy, the core porosity is usually lower. This is because the methods used to measure the porosity of the cores uses imbibed fluids (water, mercury or gas), and these fluids can only access open pore spaces: there will always be some pore spaces that are isolated and cannot be accessed.

The difference between f_t and f_e is the fraction of water held by absorbing capillary forces in the clay fraction of the rock. This amount of water can be appreciable depending upon the type and distribution of the clay, and the salinity and pH of the formation fluid. The water is bound, and does not take part in fluid flow. It is common, therefore, to ignore this water fraction and to prefer to use f_e as a representative porosity for the rock. However, one must be cautious in using the effective porosity in calculations involving resistivity tools.

The NMR tool is sensitive to the difference between bound and free water (i.e., water associated with $(f_t - f_e)$ and f_e, respectively), and can be used to derive these values directly, and then use them to predict the permeability of the rock.

20.2.3 Sand/Shale Modes

The effect on the effective porosity of the different clay modes is shown in Fig. 20.4. The clean water-bearing sand has an effective porosity of 30%, and is given by point Sd on the density-neutron crossplot (Fig. 20.4). If 10% shale is added to the sand, then the point will plot in slightly different places on the density-neutron crossplot depending upon the type of clay distribution (the mode of the shale).
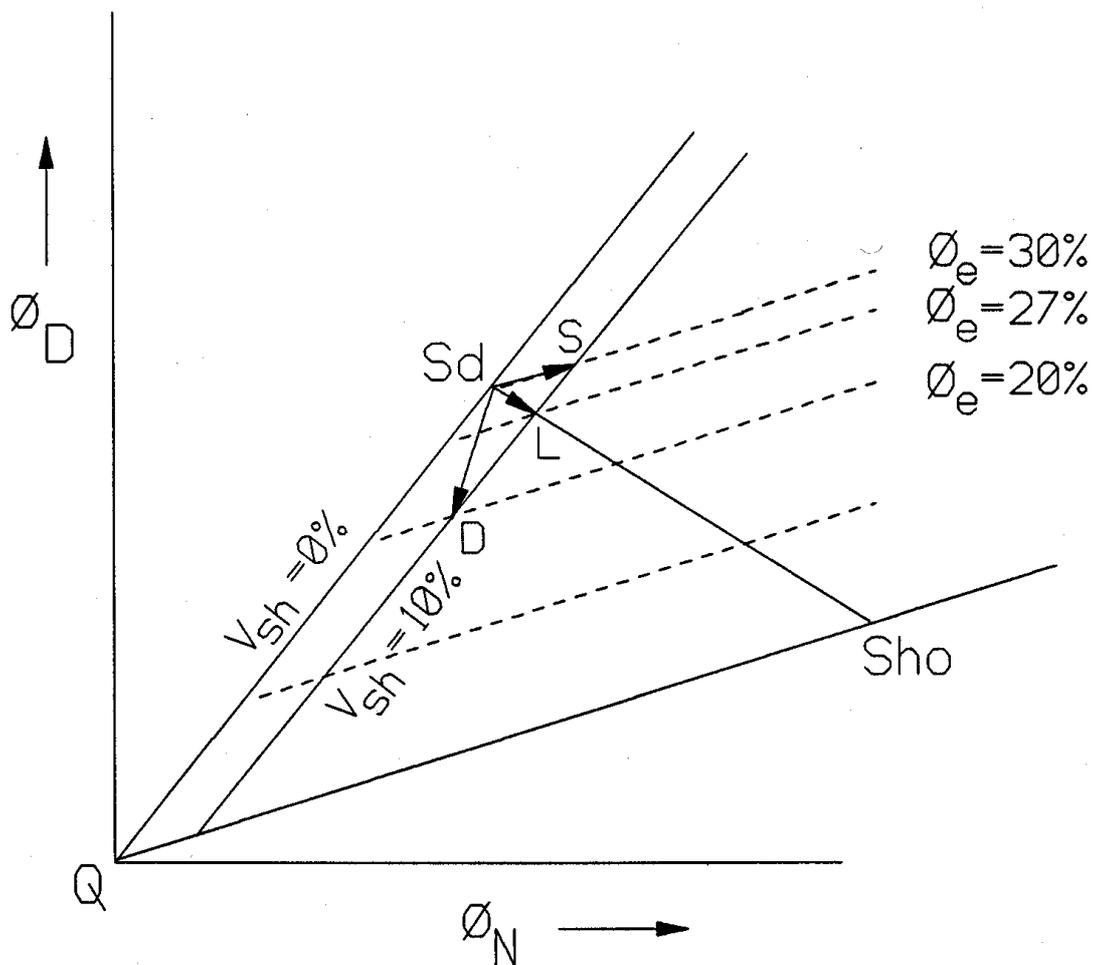
Fig. 20.4 Effect of shale/clay mode on the effective porosity of a shaly sand.

- If it is as a dispersed shale/clay, the 10% additional clays take the place of porosity, so the new effective porosity becomes 30 - 10 = 20%, and the point now plots at point D in the figure.

- If it is a laminated shale, the 10% additional clays reduce the overall effective porosity by 10%, so the new effective porosity becomes 30 – (30×10/100) = 27%, and the point now plots at point L in the figure.

- If it is a structural shale, the 10% additional clays replace volume for volume 10% of the original quartz grains, and the effective porosity is unchanged at 30%. Hence the new point plots at point S in the figure.

We can use these relationships to look at structural clay/shale distribution patterns on the density-neutron cross-plot.

Clay distribution patterns, indicating dispersed, laminated and structural shales can be analyzed with the density and neutron log data (Fig. 20.5). In this figure:
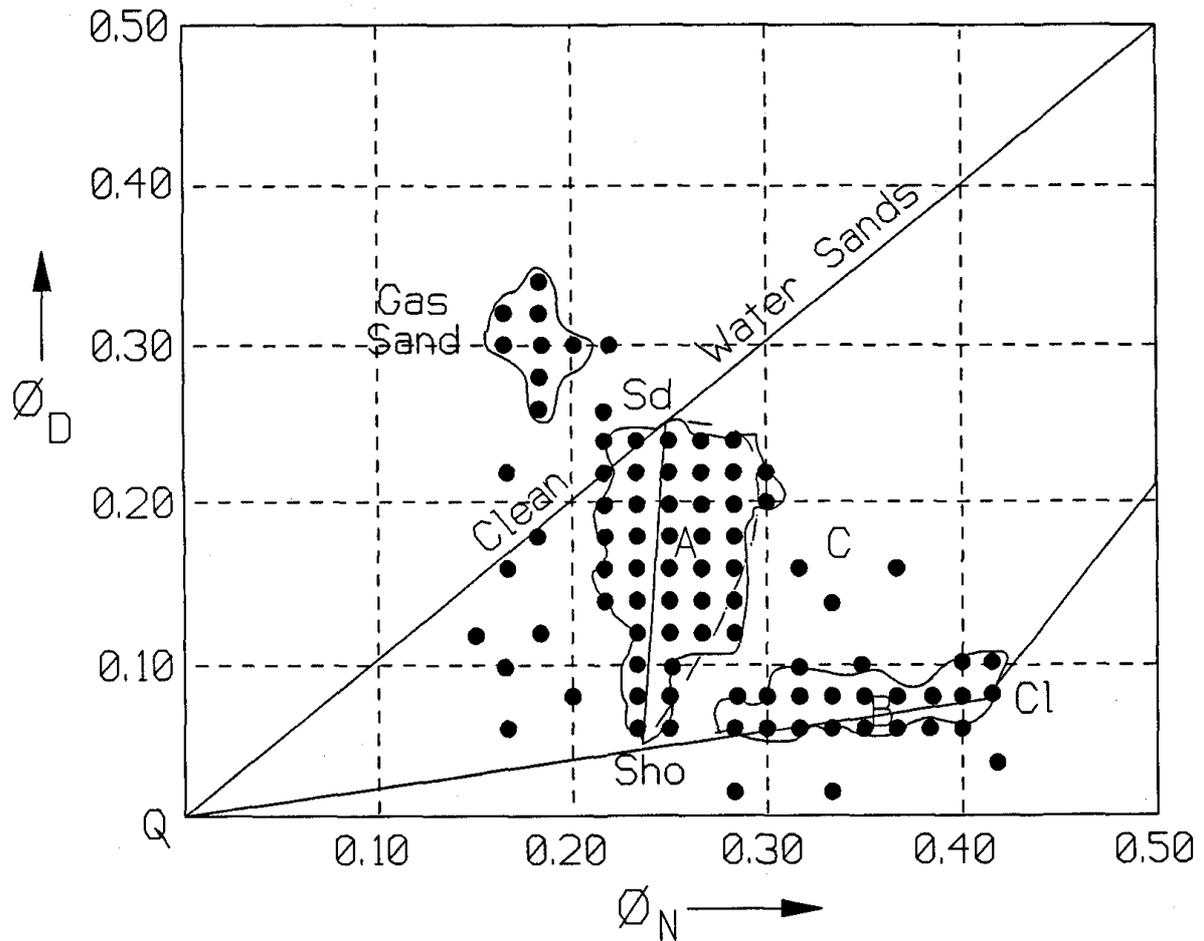
Fig. 20.5 Density-neutron crossplot showing characteristic points for shaly sands and shales.

- Cl is the "shale point" and indicates wet shale.
- The area A indicates sand and shaly sands. In area A, the samples range from clean sands at Sd to shales at point Sho.
- Laminar shales fall on the Sd-Sho line.
- Dispersed shales fall to the left of the Sd-Sho line.
- Structural shales fall to the right of the Sd-Sho line.
- The dashed line indicates the upper limit to shaly sands of laminated plus structural shale content.
- The area B indicates shales. The spread in this group is caused by the composition of the shales (composed of different clay minerals, silt and water). Pont Cl corresponds to shales which are relatively silt free, while point Sho represents shales that contain the maximum amount of silt.
- The area C indicates intermediate and ambiguous data.

If both the dry clay point and the wet clay point can be established, both the total and the effective porosities can be derived from the density and neutron log data. An example of this is shown in Fig. 20.6, which is a density-neutron cross-plot showing both the dry and wet clay points. In this case the dry clay density is assumed to be the same as that of quartz (2.65 g/cm^3) and the dry clay neutron porosity has been assumed (guessed). Both the density and the neutron porosity for the wet clay point have been taken from the log readings in adjacent good shales. Most dry clays have a density in the range 2.65 to 2.85 g/cm^3. Figure 20.9 can then be used to derive both the total and effective porosities from the density and neutron log readings in the formation of interest.
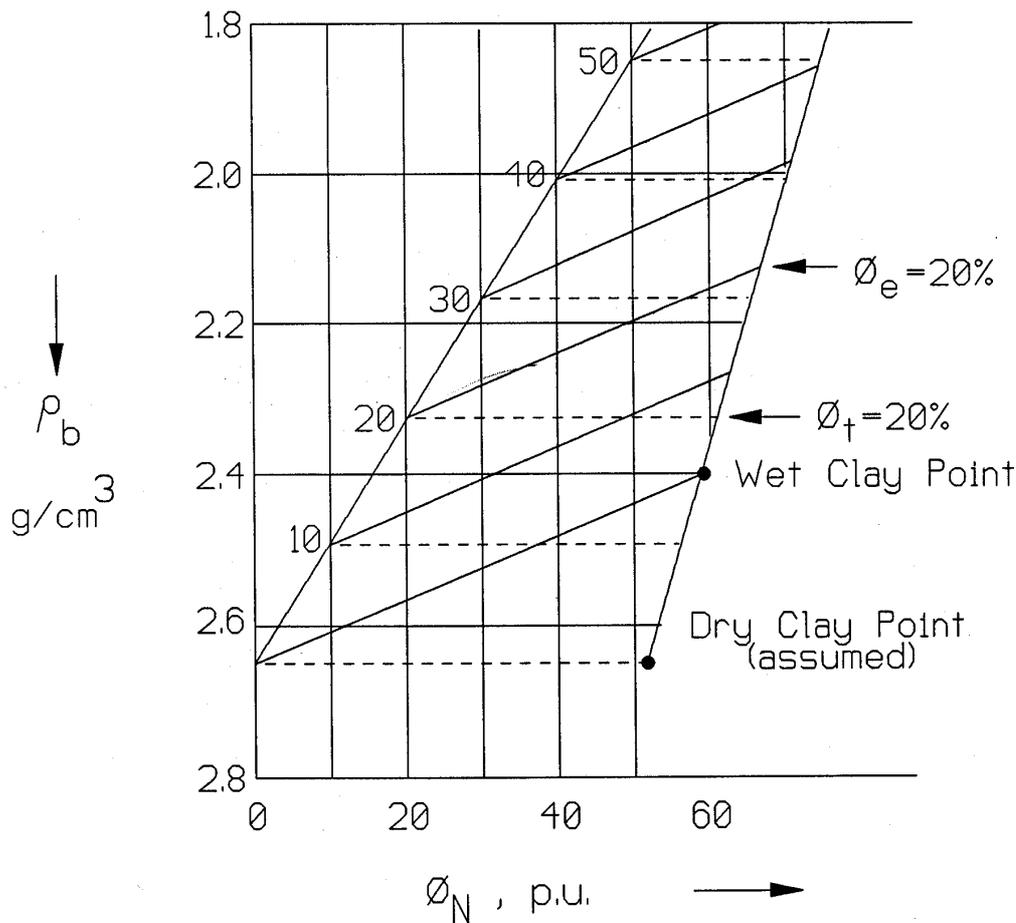
Fig. 20.6 The use of the density-neutron crossplot to calculate both total and effective porosities in shaly sands.

20.3 Resistivity Logs

The presence of clays reduce resistivity, and hence decrease the apparent hydrocarbon saturation. Their presence must be accounted for otherwise all our STOOIP calculations will be underestimated. The degree of effect that the presence of clays have depend on their amount (V_{sh}) and their distribution. Each of the tree different distributions of clay outlined above (laminar, structural, and dispersed) has a different effect upon the resistivity, SP, and sonic logs, and influences the permeability and water saturation in a different way. We can schematically illustrate the different modes of clay distribution in Fig. 20.1.

20.3.1 Laminar clays

These are thin streaks of clay deposited between units of reservoir rock. They do not change the effective porosity, the water saturation or the horizontal permeability of the reservoir layer, but destroy vertical permeability between reservoir layers.

The resistivity of the reservoir rock is the sum of the conductivities of the clean sand layers and the shale laminae:

$$C_t = C_{sand} + C_{sh} \tag{20.3}$$

or in terms of resistivity:

$$\frac{1}{R_t} = \frac{(1-V_{sh})}{R_{sand}} + \frac{V_{sh}}{R_{sh}} \tag{20.4}$$

where: $R_t =$ log reading in the borehole corrected for bed thickness and invasion.
$R_{sand} =$ resistivity of the clean reservoir rock ($R_{sand} = F_{sand}\, R_w\, S_w^{-n}$).
$R_{sh} =$ resistivity of the clay.
$V_{sh} =$ clay fraction.

Equation (20.4) can be written:

$$\frac{1}{R_t} = \frac{(1-V_{sh})\, S_w^n}{F_{sand}\, R_w} + \frac{V_{sh}}{R_{sh}} \tag{20.5}$$

which can be rearranged for water saturation:

$$S_w = \left[\left(\frac{1}{R_t} - \frac{V_{sh}}{R_{sh}} \right) \frac{F_{sand}\, R_w}{(1-V_{sh})} \right]^{1/n} \tag{20.6}$$

In practice the water saturation is found using an iterative method. The shale volume (V_{sh}) is derived from the GR or SP logs.

20.3.2 Dispersed Clays

These show very different properties from laminar shales. The permeability is significantly reduced because clays occupy the pore space and the water wetness of clays is generally higher than that of quartz. The result is an increased water saturation and a decreased fluid mobility.

There are many shaly-sand water saturation equations that have been proposed in the literature for dispersed clay systems. The most common is the Simandoux equation:

$$S_w = \left[A\,R_w\,f^{-m} \left(\frac{1}{R_t} - \frac{V_{sh}\,S_w}{R_{sh}} \right) \right]^{1/n}$$

(20.7)

This equation is also solved iteratively.

20.3.3 Structural Clays

These have similar general properties to laminar clays, as they have been subjected to the same constraints. However, they behave more like dispersed clays in respect of their permeability and resistivity properties.

20.3.4 Waxman and Smits Equation

Clay-bearing rocks have a lower resistivity because clays have a low resistivity. This is caused partly by the presence of effective surface conduction processes on their surfaces, and partly because they generally have large surface areas upon which surface conduction can take place. Waxman and Smits used this to create an alternative way of analyzing the electrical resistivity of shaly sands.

[*Note: The Waxman and Smits method is an empirical one, and is therefore a local approximation. Recently, the physics behind the double layer conduction in rocks has been solved analytically, enabling this analysis to be carried out accurately now. However, the oil industry does not yet use this method because it is new and also strongly mathematical.*]

Waxman and Smit's equation relates the electrical resistivity of a water saturated shaly sand to the water conductivity and the cation exchange capacity per unit pore volume of the rock, Q_v (meq/ml). It is this last factor that partly controls the size of the surface conduction. The method is *independent* of clay distribution.

The conductivity of the shaly water-bearing sand is expressed by:

$$C_O = \frac{1}{F^*} \left(C_w + C_s \right)$$

(20.8)

where: $F^* =$ the formation factor in shaly sand (determined at high fluid salinities).
   $C_o =$ $1/R_o$
   $C_w =$ $1/R_w$
   $C_s =$ The specific surface conductance of the clay fraction.

The value of $C_s = B \times Q_v$, where B is the equivalent conductance of the counterions as a function of solution conductivity, C_w. The units of B are Ωcm/m.meq. Equation (20.8) is represented graphically in Fig. 20.7.
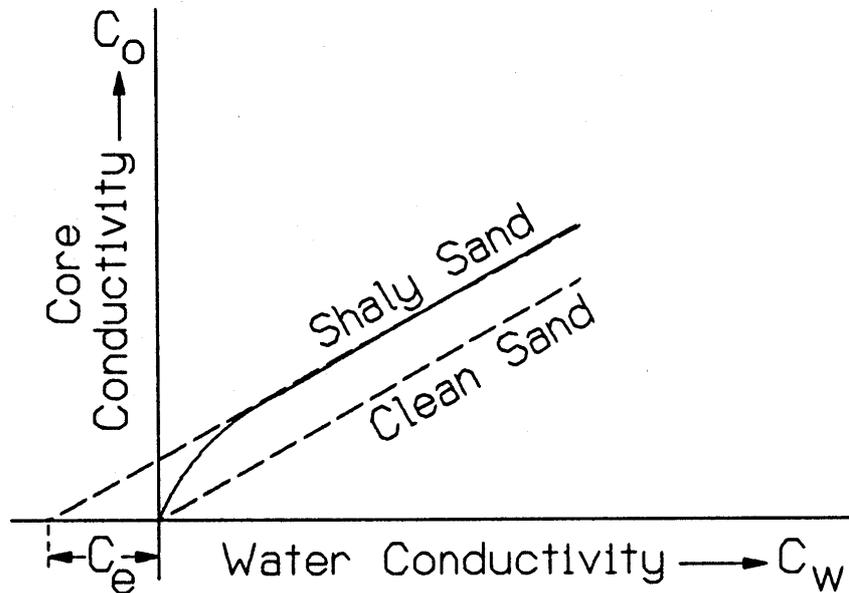
Fig. 20.7 The conductivity of a shaly sand as a function of formation water conductivity.

Since we can write $F^* = f^{m*}$, Eq. (20.8) can be rewritten:

$$R_O = \frac{f^{-m^*}}{C_w + B\,Q_v} = \frac{R_w\,f_t^{-m^*}}{1 + R_w\,B\,Q_v} \tag{20.9}$$

in which formula the triple product $R_w B Q_v$ is dimensionless.

This equation was developed and tested in the laboratory using the total porosity, and hence it should be restricted to use with total porosity.

The concentration of clay counterions as defined by Q_v can be determined in the laboratory on material from core by a titration/conductivity method. This is done on crushed samples, so there is some concern that the value may not be relevant for whole rocks. Clearly there will be more exchangeable counterions possible in crushed samples, which have a higher surface area for reactions. Some whole rock measurements exist, but are uncommonly used in the oil industry.

It has been noted that there exists in some areas a relationship between Q_v and f_t. If this is noted in a reservoir (Fig. 20.8), the Q_v value may be determined from the total porosity from log data. In shaly sands Q_v usually ranges between 0.01 and 2 meq/ml.

Empirical relationships between B and R_w have been established at different temperatures. between 50°C and 200°C (120 – 390°F) the product BR_w is not dependent upon temperature, and can be represented as a function of water salinity alone, as illustrated in Fig. 20.9.
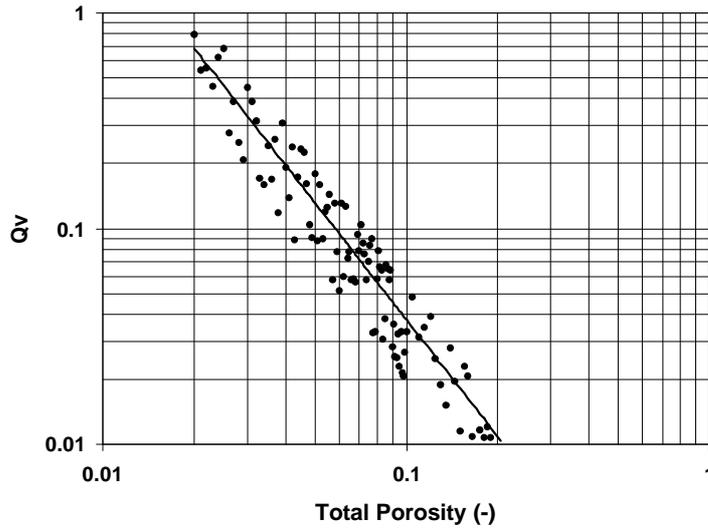
Fig. 20.8 Typical Q_v - f_t for reservoir intervals. Here Qv = 0.0006×$f_t^{-1.8}$.
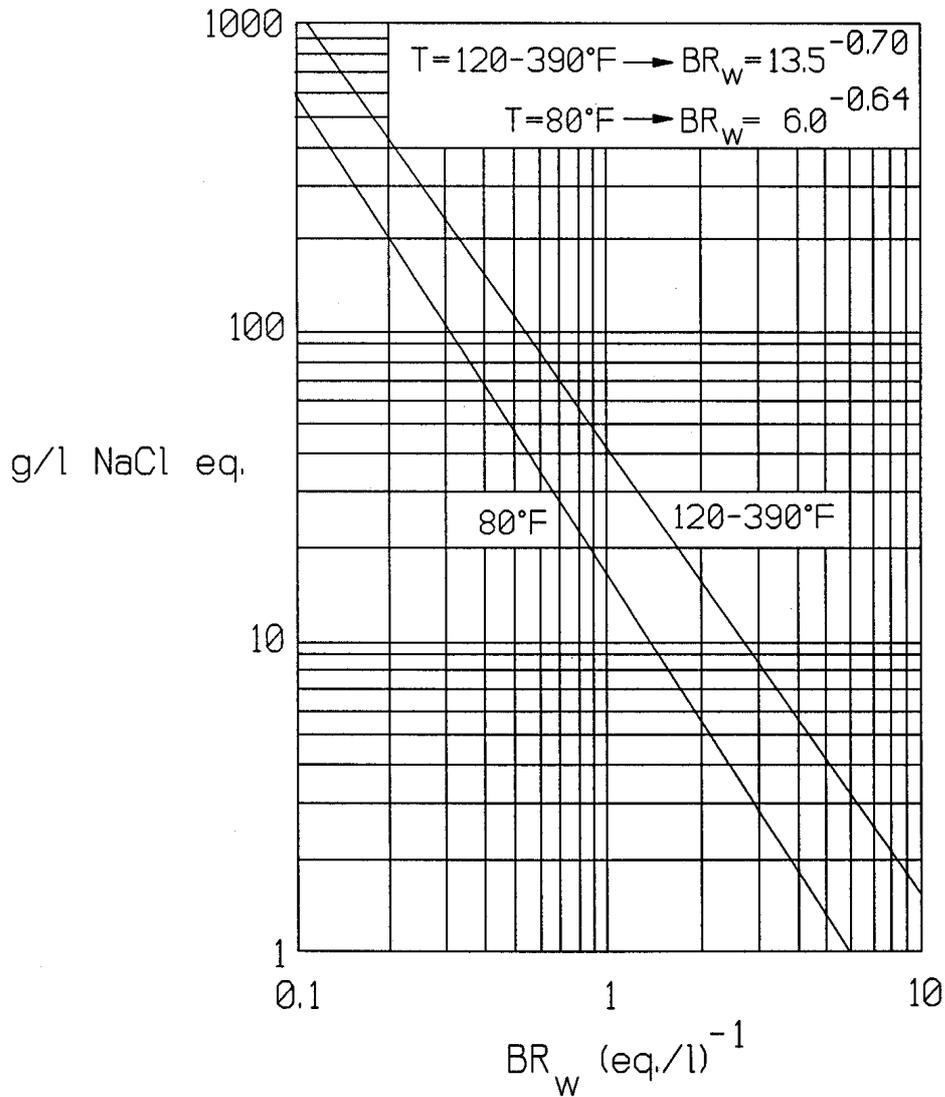
Fig. 20.9 The BR_w – Salinity relationship.

In hydrocarbon-bearing formations the exchange ions associated with the clay become more concentrated in the remaining pore water. This concentration Q_v' is related to Q_v and the water saturation S_w by $Q_v' = Q_v / S_w$.

The conductivity of the counterions is BQ_v/S_w (Ωm), hence:

$$C_t = \frac{1}{G*}\left(C_w + \frac{BQ_v}{S_w}\right)$$

(20.10)

Here, $C_t =$ the conductivity of a partially water saturated sand.

$G* =$ a geometric factor, which is a function of the porosity, water saturation and pore geometry, but independent of Q_v.

Dividing Eq. (20.8) by Eq. (20.10) gives:

$$S_w^{-n*} = \frac{G*}{F*} = \frac{R_t}{R_o} \cdot \frac{C_w + BQ_v/S_w}{C_w + BQ_v} = \frac{R_t}{R_o} \cdot \frac{1 + R_w BQ_v/S_w}{1 + R_w BQ_v}$$

(20.11)

where, $n*$ is the saturation exponent for shaly sand.

The equation is solved for S_w using an iteration process, computationally. A quick manual solution can be obtained from the graph shown in Fig. 20.10, which is valid for the saturation exponents, $n*=1.8$ and 2.0.

This is derived from the relationship:

$$\frac{R_t}{F* R_w} = S_w^{-n*}\left[\frac{1}{1 + R_w BQ_v}\right]$$

(20.12)

where, $F* =$ $F(1 + R_w BQ_v)$, and R_w and B are the values at 77oF.
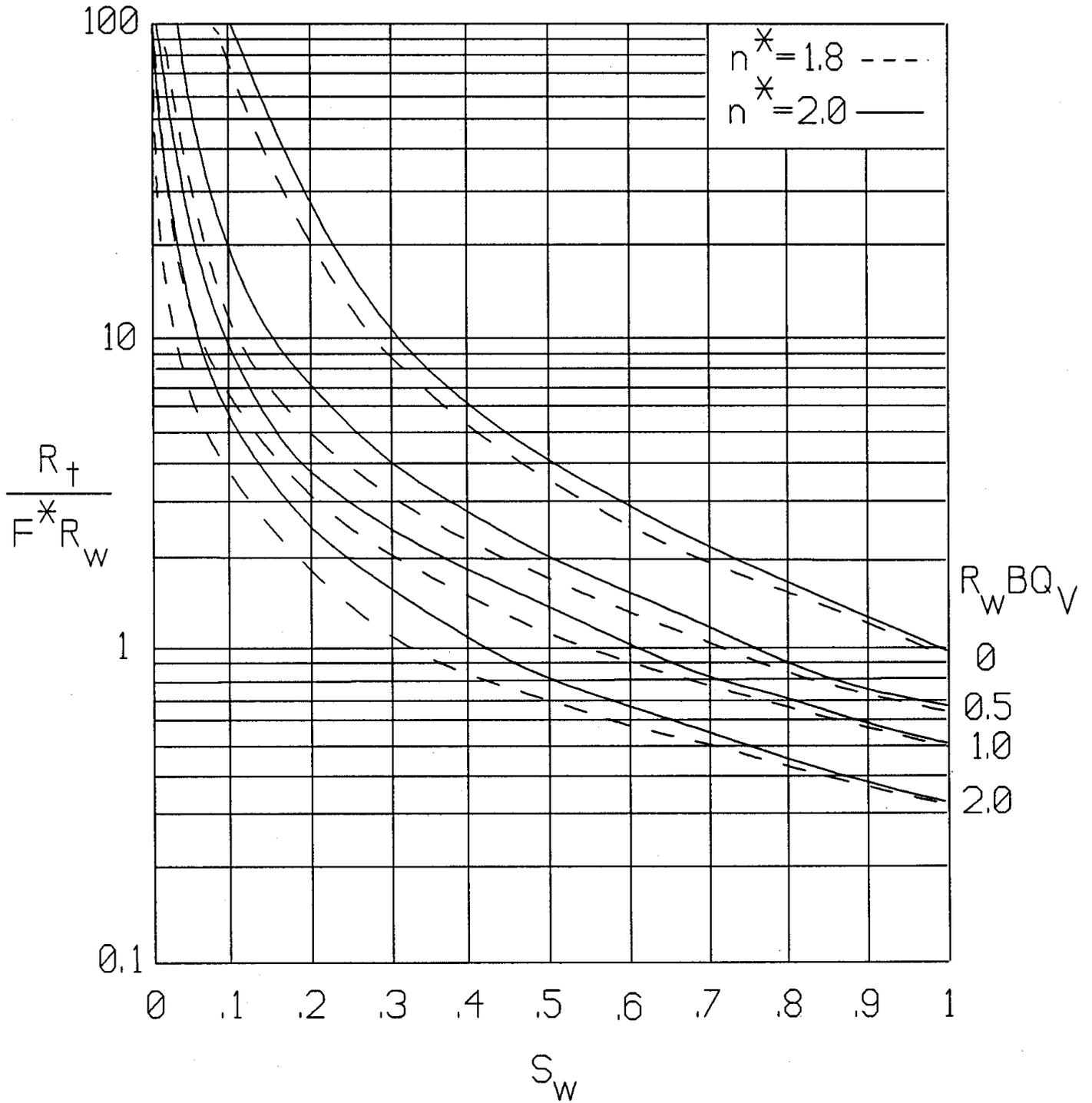
Fig. 20.10 Quick-look Waxman and Smits S_w solution chart.